Zhang *et al. Microbial Cell Factories* (2025) 24:103
https://doi.org/10.1186/s12934-025-02731-y

Microbial Cell Factories

RESEARCH Open Access

Promoting cytidine biosynthesis by modulating pyrimidine metabolism and carbon metabolic regulatory networks in *Bacillus subtilis*

Xiangjun Zhang[1], Lu Liu[2], Pilian Niu[1], Tong Ye[2], Wei Ding[2], Xiaobo Wei[2], Junnan Xu[2], Haitian Fang[2*] and Huiyan Liu[2*]

Abstract

Background The modification of single or multiple genes via metabolic engineering can lead to the dysregulation of central metabolism and affect bacterial growth and metabolite accumulation. Meanwhile, transcription factor engineering can trigger metabolic network reprogramming at the global or systemic level, redirecting metabolic flux toward the synthetic pathways of target metabolites. In this study, we modulated pyrimidine and carbon-nitrogen metabolism in *Bacillus subtilis* through transcription factor engineering to promote the synthesis of cytidine, a drug intermediate.

Results First, cytidine synthesis was enhanced by knocking out the transcriptional regulator PyrR, which increased the cytidine titer during shake flask fermentation to 0.67 g/L. Second, mutations in the transcriptional regulator catabolite control protein A (CcpA) significantly promoted cytidine synthesis, increasing the shake flask titer to 2.03 g/L. Finally, after culture in a 5 L fermenter, the cytidine titer reached 7.65 g/L, which was 3.77-fold that of shake flask fermentation. Moreover, a cytidine yield and productivity of 0.06 g/g glucose and 0.16 g/L/h, respectively, were achieved. Subsequently, the regulatory mechanisms through which PyrR and CcpA modification affect cytidine biosynthesis were explored through multi-omics analysis. Transcriptome and metabolome analysis revealed that coordinated alterations in carbon, nitrogen, nucleotide, and amino acid metabolism were essential to promote cytidine synthesis. However, the increased cytidine production in recombinant strains was attributed to the enhancement of pyrimidine metabolism, the Phosphotransferase (PTS) system, the tricarboxylic acid (TCA) cycle, the pentose phosphate (PP) pathway, and nitrogen metabolism.

Conclusions These results indicate that PyrR knockdown can enhance pyrimidine metabolic pathway and promote cytidine synthesis. CcpA mutation can reprogram the central carbon-nitrogen metabolic network, change the metabolic flow to *de novo* synthesis pathway of pyrimidine nucleoside, increase the supply of cytidine synthesis

*Correspondence:
Haitian Fang
fanght@nxu.edu.cn
Huiyan Liu
liuhy@nxu.edu.cn

Full list of author information is available at the end of the article

precursors and promote the accumulation of cytidine. Overall, regulation of engineered carbon and nitrogen metabolic networks is essential for improving the efficiency of microbial cell factories.

Keywords Cytidine, Transcription factor engineering, Catabolite control protein A (CcpA), Transcriptome, Metabolome

Introduction

Cytidine is a valuable intermediate in the synthesis of antiviral and antineoplastic drugs and is widely used in the pharmaceutical industry and the nutraceutical and healthcare sectors [1–3]. In recent years, the production of cytidine using metabolically engineered or mutant strains of bacteria — such as *Escherichia coli* [4], *Bacillus subtilis* [5] and *Bacillus amyloliquefaciens* [6] — has emerged as a more efficient alternative to traditional chemical synthesis and nucleic acid hydrolysis techniques [7]. Metabolic engineering focuses on achieving high metabolite titers and productivity in microbial cell factories while ensuring process economy [8]. In order to achieve these goals, researchers have employed various rational approaches to modify cytidine-producing strains of bacteria. These approaches have included the blockade of catabolic pathways [9], release of metabolite feedback inhibition [6, 10], enhancement of precursor supply [10, 11], transporter engineering [5, 12], and cofactor engineering [11, 13]. However, the modification of single or multiple genes often proves inadequate for achieving the desired outcomes and product yield, since such modifications can lead to metabolic pathway disorders, resulting in an imbalance between bacterial growth and product accumulation [14]. With advancements in functional genomics, transcription factors (TFs) have been recognized as essential tools for reshaping metabolic pathways due to their unique capacity for "multifaceted regulation," addressing the limitations associated with single-gene modifications. Meanwhile, as TFs are integral components of gene regulation, their modifications can trigger the reprogramming of metabolic networks at both the global and systemic levels, facilitating the redirection of metabolic flux toward the synthetic pathways of target products [15, 16]. Recent studies have employed TFs engineering methods to reconstruct carbon-nitrogen metabolism in various microbial strains, thereby enhancing the production of compounds such as extracellular enzymes, industrial chemicals, and heterologous proteins [17, 18]. Nevertheless, there is a notable paucity of research focused on improving pyrimidine nucleoside synthesis through TFs engineering strategies.

In *B. subtilis*, the *de novo* synthesis pathway of pyrimidine nucleosides is primarily regulated by the pyrimidine operon (pyr operon), which consists of ten genes that encode a total of eight enzymes [19]. Among these genes, eight code for six enzymes that participate in the *de novo* synthesis of cytidine. Notably, the *pyrR* gene encodes a repressor protein that regulates the expression of the pyr operon itself [19]. For example, when repressor PyrR bind to specific regulatory sequences (binding loops, BLs), the transcription of the pyr operon genes (*pyrAA/AB/B/C/D/E/F/K*) is inhibited. Conversely, when PyrR binds to 5-phosphoribosyl-1α-pyrophosphate (PRPP) but not to the downstream BLs, the pyr operon genes undergo normal transcription. A study conducted by Zhu et al. demonstrated that the knockout of *pyrR* significantly enhances the expression levels of pyr operon genes, resulting in increased uridine biosynthesis [5]. Similarly, Wang et al. reported that modifying the pyr operon can attenuate the regulatory influence of the PyrR protein [20]. CcpA is a principal TF involved in the regulation of carbon and nitrogen metabolism in *B. subtilis*. This TF is known to regulate approximately 300 genes, including those encoding enzymes responsible for the transport and utilization of carbon sources (*bglP*, *ptsH*, *glpF*, *amyE*, *amyO*, *pfkA*, *gapA*, *pdhA*, *gntR*), short-chain fatty acid (SCFA) metabolism (*ackA*, *pta*, *acsA*, *acuABC*), the PP pathway (*zwf*, *pgl*, *rpe*, *purA*), the TCA cycle (*citB*, *citZ*), branched-chain amino acid synthesis (*asnB*, ilv-leu operon), and nitrogen metabolism, e.g. glutamate dehydrogenase (GDH), glutamate synthase (GOGAT) and glutamine synthetase (GS) (*rocG*, *gudB*, *glnA*, *gltAB* operon), which is essential for ammonium assimilation [21–24]. Both PyrR and CcpA play crucial roles in coordinating pyrimidine nucleotide metabolism as well as carbon and nitrogen metabolism in *B. subtilis*.

In this study, we used the recombinant strain BSNX2 obtained by knocking out the cytidine deaminase and uridine kinase coding genes *cdd* and *udk* to block the cytidine degradation pathway as the starting strain. We investigated the influence of the regulators of pyrimidine nucleoside metabolism (PyrR) and carbon and nitrogen metabolism (CcpA) on cytidine production in *B. subtilis*. Our findings revealed that the cytidine titer in the *pyrR* knockout strain (BSNX3) increased, while the titer in the *ccpA* knockout strain decreased, along with reductions in sugar consumption and biomass. Consequently, a mutation library based on the D1 and D2 domains of *ccpA* was constructed, leading to the identification of a recombinant strain, BSNX4-DM, which exhibited a significantly increased cytidine titer. To elucidate the mechanisms by which PyrR and CcpA regulate cytidine synthesis, we performed transcriptomic and metabolomic analyses on the recombinant strains.

Materials and methods

Strains, plasmids and cultures

All strains and plasmids used in this study are listed in Table 1. *E. coli* DH5α was used as the intermediate cloning host for plasmid construction, and transformed clones were screened using kanamycin (50 μg/mL). *B. subtilis* was cultured aerobically in LB medium or on LB agar plates at 37℃, and kanamycin was added to the medium for screening. We prepared and electrotransformed *B. subtilis* competent cells according to the protocol described by Anagnostopoulos and Spizizen [25] and Jin et al. [26].

Construction and expression of recombinant plasmids

Recombinant plasmids were assembled using the method described by Ferrando et al. and Altenbuchner [27, 28]. All primers used are listed in Supplementary Table 1. The plasmid pJOE8999 was linearized using the restriction enzyme *BsaI*, and PyrR-sgRNA and CcpA-sgRNA sequences were introduced into the linearized plasmid to obtain the pJOE8999-PyrR-sgRNA and pJOE8999-CcpA-sgRNA recombinant plasmid. With the genome of the BSNX2 strain as a template, the upstream and downstream homology arms of the *pyrR* and *ccpA* genes were amplified using the primer pairs PyrR-U-F/PyrR-U-R, PyrR-D-F/PyrR-D-R, CcpA-U-F/CcpA-U-R, CcpA-D-F/CcpA-D-R containing *SfiI* restriction sites, respectively. Then, the upstream and downstream homologous arms of the *pyrR* and *ccpA* genes were ligated into a sequence via overlap extension PCR, and pJOE8999-PyrR-sgRNA and pJOE8999-CcpA-sgRNA plasmids linearized by restriction endonuclease *SfiI* were introduced to obtain the recombinant plasmid pJOE8999_PyrR and pJOE899_CcpA. The recombinant plasmid was transformed into the BSNX2 strain via electrotransformation, and the recombinant strains BSNX3 and BSNX4 was obtained.

Table 1 Strains and plasmids used in this study

Name	Characteristics	Source
Strains		
B. subtilis 168	Wild type	Laboratory stock
BSNX2	*Bacillus subtilis* 168 derivate, Δ*cdd*, Δ*udk*	Laboratory stock
BSNX3	*Bacillus subtilis* 168 derivate, Δ*cdd*, Δ*udk*, Δ*pyrR*	This work
BSNX4	BSNX3 derivate, Δ*ccpA*	This work
BSNX4-DM	BSNX3 derivate, *ccpA* mutant E43D/S77A/M103L/S281A/P314K	This work
Plasmids		
pJOE8999	Contains CRISPR-Cas9 system plasmid for breaking genome, Kan^r	[27]
pUC19	[*EcoRI-HindIII*] Linearized Vector	Laboratory stock
pJOE8999-Δ*pyrR*	pJOE8999-derivation with deletion gene of *pyrR*	This work
pJOE8999-Δ*ccpA*	pJOE8999-derivation with deletion gene of *ccpA*	This work
pJOE8999-$CcpA^M$	pJOE8999-derivation with mutation gene of *ccpA*	This work

The recombinant strains stored at -80℃ were inoculated on LB plates and cultured at 37℃ for 12 h. The seed medium components were as follows (g/L): glucose, 20; Yeast powder, 10; Peptone, 5; NaCl, 2.5; $MgSO_4 \cdot 7H_2O$, 1; KH_2PO_4, 2; Sodium glutamate, 1.5. The shake flask fermentation medium components were as follows (g/L): glucose, 80; Peptone, 10; Yeast powder, 15; NaCl, 2.5; $MgSO_4 \cdot 7H_2O$, 3; KH_2PO_4, 2.5; $(NH_4)_2SO_4$, 6; Sodium glutamate, 5. The pH value of the seed and fermentation medium was 7.0. Single colonies of recombinant strains on LB plates were picked and inoculated into 100 mL triangular flasks containing 10 mL of seed medium, and cultured overnight at 37 °C and 200 rpm with shaking. The seed culture was inoculated into a 500 mL flask containing 50 mL of fermentation medium and cultured at 37 °C, 200 rpm for 48 h. The fermentation broth was collected to detect the OD_{600} value and cytidine titers. Based on the fermentation curve, an appropriate time point was selected to collect samples for transcriptome (logarithmic growth phase) and metabolome (logarithmic growth phase) analysis. By analyzing the changes in gene expression levels and metabolite contents in the recombinant strains, the effects of modification of transcriptional regulators PyrR and CcpA on metabolic pathways related to cytidine biosynthesis were explored.

CcpA homologous sequence alignment and construction of mutation library

In the MEME Suite (http://meme-suite.org/) website [29], the CcpA protein sequence of *Bacillus subtilis* 168 (NP_390852.1) was homologously compared with nine other CcpA protein sequences, including CcpA (*Bacillus spizizenii*) (WP_019715392.1), CcpA (*Bacillus halotolerans*) (WP_024122513.1), CcpA (*Bacillus inaquosorum*) (WP_003237907.1), CcpA (*Bacillus amyloliquefaciens*) (WP_289393829.1), CcpA (*Bacillus atrophaeus*) (WP_010789522.1), CcpA (*Bacillus licheniformis*) (WP_003184445.1), CcpA (*Bacillus wiedmannii*) (WP_001103309.1), CcpA (*Bacillus cereus*) (WP_001103303.1) and CcpA (*Bacillus thuringiensis*) (WP_001103303.1).

To obtain CcpA that promotes cytidine synthesis, two CcpA mutation libraries (D1 and D2 domains) were constructed. With the BSNX3 genome as the template, the 1.5-kb *ccpA* sequence was amplified using the targeted mutation primers CcpA-D1-F/CcpA-D2-R and CcpA-D2-F/CcpA-D2-R and inserted into pUC19 (pUC19-CcpA). Subsequently, linearized plasmids were obtained through PCR amplification using pUC19-CcpA as template and CcpA-F/R as primer. These plasmids were

treated with polynucleotide kinase to phosphorylate the 5' end. DpnI endonuclease was used to remove any circular DNA, and the plasmid was then transformed into DH5α cells following cyclization with T4 DNA ligase. Finally, the *ccpA*-targeted mutant fragment was ligated between the *SfiI* site of the pJOE8999-CcpA-sgRNA plasmid to obtain the recombinant plasmid pJOE8999-CcpA^{M}. The *ccpA* gene mutation library was obtained following electrotransformation into the mutant BSNX3. The *ccpA* gene mutant in the domain D1 mutation library carries a mutation site, 43E; The D2 domains of the *ccpA* gene contained four mutation sites, 77 S/103 M/281S/314P. These five amino acids could be mutated into any combination of random amino acids.

High-throughput screening of *CcpA* gene mutation library

Mutant screening was performed using a previously described high-throughput screening method [4, 30]. First, the cultured mutants were transferred into a 96-well plate containing 200 μL seed culture medium and incubated at 37 °C, 220 rpm for 12 h. Then, an appropriate amount of culture was inoculated into a 96-well plate containing 200 μL fermentation culture medium, and continued to be cultured at 37 °C, 220 rpm for 48 h. After fermentation, the supernatant was collected via centrifugation, diluted, and transferred to a 96-well plate, and the absorbance of each well was measured at 270 nm using a microplate reader. The cytidine content (g/L) was evaluated according to the following equation: Cytidine content = (OD_{27} − 0.019472)/1.5386. The screened mutants with the highest cytidine titer were used for shake flask fermentation and validation experiments.

Transcriptomics analysis

BSNX2, BSNX3 and BSNX4-DM strains were collected during the logarithmic growth phase of shake flask fermentation and rapidly frozen in liquid nitrogen. The samples were sent to Novogene (Beijing, China) for the extraction of total RNA, and the RNA integrity and quantity were accurately detected using an Agilent 2100 bioanalyzer. Transcriptome sequencing was performed on the Illumina HiSeq-4000 sequencing platform. The analysis of gene expression was performed using DESeq2 [31], and the screening criteria for differentially expressed genes (DEGs) were $|\log_2 FC| > 1.2$ and $p_{adj} < 0.05$ [32]. DEGs were further analyzed based on Gene Ontology (GO) and Kyoto Encyclopedia of Genes and Genomes (KEGG) enrichment.

Metabolomics analysis

The culture in the logarithmic growth phase was centrifuged to collect the supernatant, which was quickly frozen in liquid nitrogen for metabolite extraction. Subsequently, the extraction buffer (CAN: methanol = 1:4, v/v) was added to the sample, and the supernatant was collected via centrifugation for liquid chromatography coupled with mass spectroscopy. With a 0.1% formic acid aqueous solution (A) and 0.1% formic acid acetonitrile solution (B) as the mobile phase, the samples were analyzed using a UHPLC system (LC-30 A, Shimadzu) coupled with a Waters ACQUITY Premier HSS T3 Column and a TripleTOF 6600+ mass spectrometer (SCIEX, Foster City, CA, USA). Analyst TF 1.7.1 Software was employed for data acquisition. ProteoWizard was used to convert the original data into the mzXML format [33], and peak extraction, alignment, and retention time correction were performed using the XCMS program [34]. In this study, VIP > 1.2 & *p*-value < 0.05 (Student's t-test) were used as the criteria to identify differential metabolites. Further functional annotation and pathway enrichment analysis were performed using the KEGG database.

Real-time quantitative PCR (RT-qPCR) analysis of gene transcription level

The strains cultured to the logarithmic growth phase were centrifuged at 4000×*g* and lower temperature to collect bacterial pellets. Then, total RNA was extracted according to the procedure described in the reagent kit (OMEGA, R6950-01), and the reverse transcription kit (Vazyme, R333-01) was used to synthesize cDNA according to the manufacturer's instructions. Subsequently, RT-qPCR was performed according to the kit instructions (Vazyme, Q711-02), and data analysis was performed using the qTOWER^{3}G PCR system. The 16 S rRNA gene was employed as the reference gene; the RT-qPCR primers are shown in Supplementary Table 1. Data processing was performed using the $2^{-\Delta\Delta Ct}$ method [35], and at least three replicates were examined for each sample.

Fed-batch culture in a 5 L bioreactor

The strains BSNX4-DM with the best production performance were cultured in a fed-batch 5 L bioreactor (Bailun, Shanghai, China). The components of fed batch fermentation medium (g/L): glucose, 80; Yeast powder, 20; $(NH_4)_2SO_4$, 5; KH_2PO_4, 1; K_2HPO_4, 5; Sodium citrate, 10; Sodium glutamate, 20; $MgSO_4 \cdot 7H_2O$, 1.5; $MnSO_4$, 0.02; $ZnSO_4$, 0.02; the pH was adjusted to 7.0. The seed culture was inoculated into a 5 L bioreactor containing 1.2 L of fermentation medium with 5% inoculation amount. The aeration rate and stirrer speed were controlled at 1.0 vvm and 500 rpm, respectively, until the end of fermentation. The pH value was maintained at 7.0 by adding 50% ammonia water, and the temperature was maintained at 37℃. By adding 600 g/L of glucose, the glucose concentration in the fermentation broth was maintained at 5 g/L.

Table 2 Results of shake flask fermentation of different Recombinant strains

Strains	OD_{600}	Cytidine (g/L)	Yield (g/g glucose)	Productivity (g/L/h)
BSNX2	10.57 ± 0.35	0.32 ± 0.02	0.014 ± 0.002	0.007 ± 0.001
BSNX3	10.21 ± 0.27	0.67 ± 0.04**	0.031 ± 0.004**	0.014 ± 0.002**
BSNX4	8.05 ± 0.19**	0.50 ± 0.02*	0.023 ± 0.002*	0.010 ± 0.001**
BSNX4-DM	11.23 ± 0.53**	2.03 ± 0.05**	0.078 ± 0.001**	0.043 ± 0.005**

Significance represents the difference between each recombinant strain and its starting strain (BSNX3 vs. BSNX2, BSNX4 vs. BSNX3, BSNX4-DM vs. BSNX3)

Determination of cytidine, OD_{600} values, and glucose concentrations

The cytidine titer in the fermentation broth was measured using high-performance liquid chromatography (HPLC) (1260 Infinity II, Agilent) on a system equipped with an Eclipse XDB-C18 column (Agilent, USA) and a PDA detector. For HPLC, 20 mM ammonium acetate and 100% methanol (96 : 4) were used as the mobile phase at a flow rate of 1.0 mL/min at 30℃. The absorbance of the cells at 600 nm was measured using an ultraviolet spectrophotometer (Metash, Shanghai, China). The residual glucose content in the fermentation broth was detected via a biochemical sensor (SBA-40E, Shandong, China).

Statistical analysis

All data are expressed as mean ± standard deviation ($n = 3$). Two-sample t-test and one-way ANOVA were performed using SPSS 22.0 software. A p value of less than 0.05 was considered statistically significant, with * indicating $p < 0.05$ and ** indicating $p < 0.01$.

Results and discussion

Effects of transcriptional regulator (*pyrR* and *ccpA*) knockout on cytidine biosynthesis

To study the effects of PyrR and CcpA on cytidine biosynthesis, the recombinant strains BSNX3 and BSNX4 were constructed. Shake flask fermentation revealed that the cytidine titer of strain BSNX3 was 0.67 g/L, which was 109.38% higher than that of strain BSNX2 (0.32 g/L). Notably, the yield of BSNX3 was significantly improved, reaching 0.0083 g/g glucose, which was 107.5% higher than that of BSNX2 (Table 2). Without any significant change in cell growth (Fig. 1A, B). RT-qPCR revealed that the transcription levels of the pyr operon genes *pyrAA/AB/B/C/D/F/K* were significantly up-regulated in the BSNX3 strain (Fig. 1C). This indicated that the disruption of the transcriptional regulator PyrR can attenuate the transcriptional repression of the pyr operon, allowing the metabolic flux to flow toward cytidine biosynthesis, consistent with previous reports [5]. As shown in Table 2, at the end of fermentation, the cytidine titer of strain BSNX4 was 0.5 g/L, and the yield was 0.0063 g/g glucose, which was 25.37% and 24.09% lower than that of BSNX3, and the OD_{600} decreased from 10.21 to 8.05. These results indicated that knocking out the transcriptional regulator CcpA affects the transport and utilization of carbon sources in *B. subtilis*, leading to the dysregulation of central carbon metabolism and indirectly decreasing the metabolic flux of the cytidine synthesis pathway. Similar results were also observed in a *ccpA* knockout strain of *Bacillus licheniformis* [23]. To obtain mutants that promote cytidine production after the functional modification of CcpA, a CcpA domain mutation library was constructed.

Domain analysis and mutation library construction of global transcription factor CcpA

The genetic relationship after homology alignment of CcpA protein sequences is shown in Fig. 2A. The domain structure of the global transcription factor CcpA was analyzed using NCBI's CD-Search tool (http://www.ncbi.nlm.nih.gov/cdd/) [36]. The results showed that the CcpA protein consists of an N-terminal DNA-binding domain (DBD) and a C-terminal dimerization effect binding domain (DEBD) (Fig. 2B). The DBD accounts for the first 60 amino acid residues of the CcpA protein structure and contains two distinct DNA-binding elements: (i) a three-helix bundle, in which helices 1 and 2 constitute the major groove-binding helix-turn-helix motif (HTH) (helix 1: residues 5–12, helix 2: residues 16–24, helix 3: residues 31–44), and (ii) a hinge helix (helix 4; residues 50–58) that is embedded in the minor groove of the central CpG

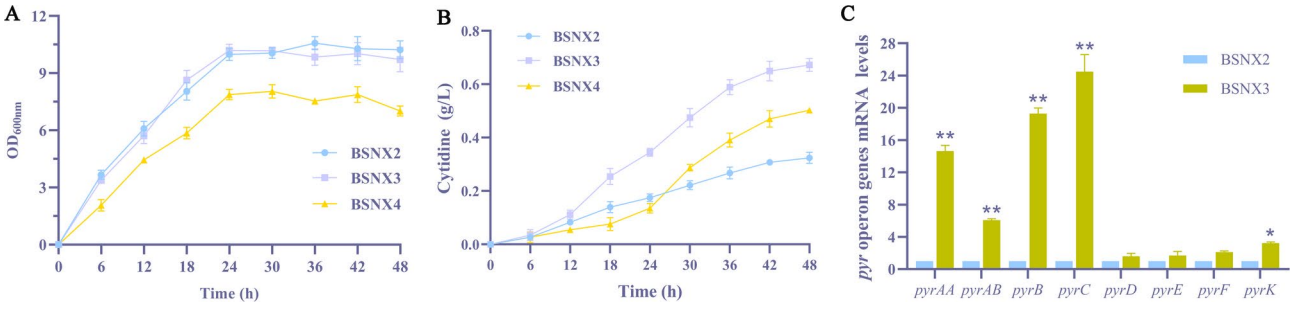

Fig. 1 Effects of transcriptional regulator (*pyrR* and *ccpA*) knockout on cytidine biosynthesis in *B. subtilis*. (**A**) Cell growth curves of different *B. subtilis* mutants. (**B**) Titers of cytidine of different *B. subtilis* mutants (**C**) The mRNA expression levels of the *pyr* operon gene in mutant BSNX3

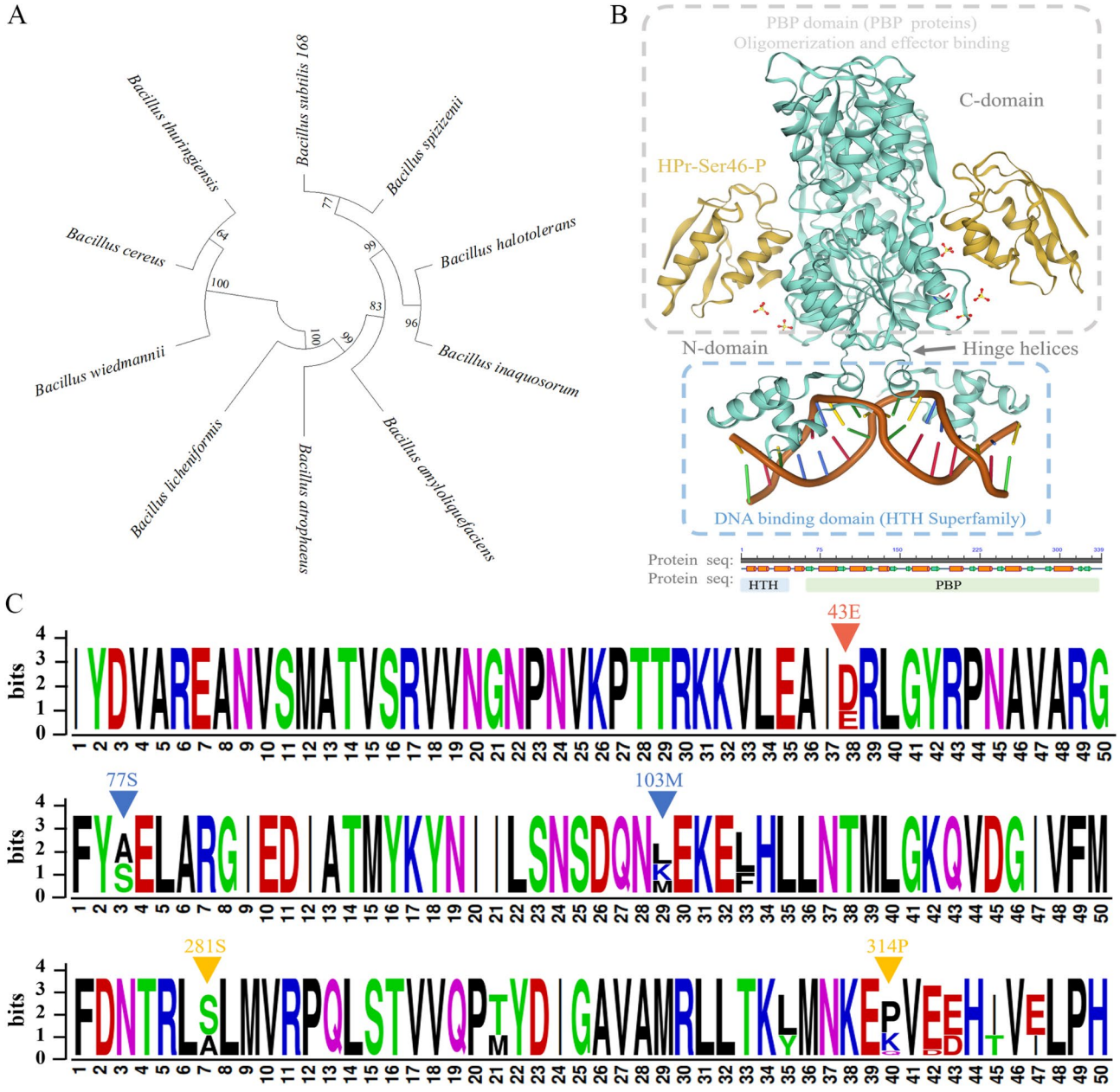

Fig. 2 Analysis of the domains of CcpA. (**A**) The homology of *B. subtilis* CcpA protein sequence and other nine CcpA protein sequences were aligned in the evolutionary tree. (**B**) The structure of CcpA with DNA molecular binding. (**C**) Sequence logos of alignment results

step and thereby introduces a kink in the DNA structure. Owing to the conformational flexibility of residues 45–50 in the HTH module and its flexible attachment with the hinge helices, the HTH motif itself demonstrates plasticity. Thus, it can optimally dock into the major groove of DNA [22, 37]. Meanwhile, the DEBD spans amino acid residues 60 to 339 and contains two structurally similar N and C subdomains. Specifically, the N subdomain consists of a six-stranded parallel β-sheet structure and four surrounding α-helices. Meanwhile, the C subdomain consists of five β-strands and five surrounding α-helices. Notably, the DEBD can bind to the Ser46-phosphorylated form (HPr-Ser46-P) of the serine-containing phosphocarrier protein (HPr) and the Ser46-phosphorylated form (Crh-Ser46-P) of the serine-containing HPr-like protein (Crh, for the catabolite repression HPr). This interaction triggers the allosteric switch of CcpA, allowing CcpA to bind to the catabolite-responsive elements (cre) site of the cognate DNA sequence [37–41]. Notably, these cre sites are composed of semi-palindromic sequences with the consensus sequence "WTGNAANCGNWNNCWW (R represents G or A, W represents A or T, N represents any base)" [42]. The location of these sites in the promoter determines whether CcpA acts as a repressor or

activator. For example, when the cre site is upstream of the promoter, CcpA acts as an activator, but when it is downstream of the promoter, CcpA acts as a repressor [43, 44].

The alignment of homologous protein sequences revealed that most of the residues within the two domains of CcpA in *B. subtilis* were highly conserved, although a few residues showed significant variations. Therefore, we constructed two mutation libraries for residues showing large interspecies differences in DBD and DEBD (Fig. 2C). In the DBD, one residue (43E) was mutated to construct a mutant library, D1. Additionally, four residues that showed considerable differences across homologous sequences (77 S/103M/281S/314P) were selected from the DEBD to construct a mutant library named D2 (Fig. 3C). Using high-throughput screening, the top 20 mutants showing the highest absorbance at 270 nm were identified from the mutation libraries D1 and D2 (Fig. 3A). The first five mutants in the mutant libraries D1 and D2 showing the highest absorbance at 270 nm were validated through shake flask fermentation experiments (Fig. 3B, C). D1-M11 (E43D) showed the highest cytidine titer of 0.995 g/L in mutant library D1. The cytidine titer of D2-M7 (S77A/M103L/S281A/P314K) in mutant library D2 was even higher at 1.37 g/L. Thus, the recombinant strain BSNX4-DM was obtained by integrating these five mutations (E43D /S77A/M103L/S281A/P314K) in the DBD and DEBD of CcpA. As shown in Table 2, compared with BSNX3, the cytidine titer of BSNX4-DM increased from 0.67 g/L to 2.03 g/L, the yield increased from 0.0083 g/g glucose to 0.0254 g/g glucose, the productivity increased from 0.014 g/L/h to 0.042 g/L/h, and the OD_{600} increased from 10.21 to 11.23.

Fed-batch culture of recombinant strain BSNX4-DM

To determine the productivity of the recombinant strain BSNX4-DM, we performed fed-batch culture in a 5 L bioreactor. As shown in Fig. 4, the early stage of fermentation was dominated by growth, and the OD_{600} peaked at 41.34 after 24 h. Cytidine synthesis was detected after

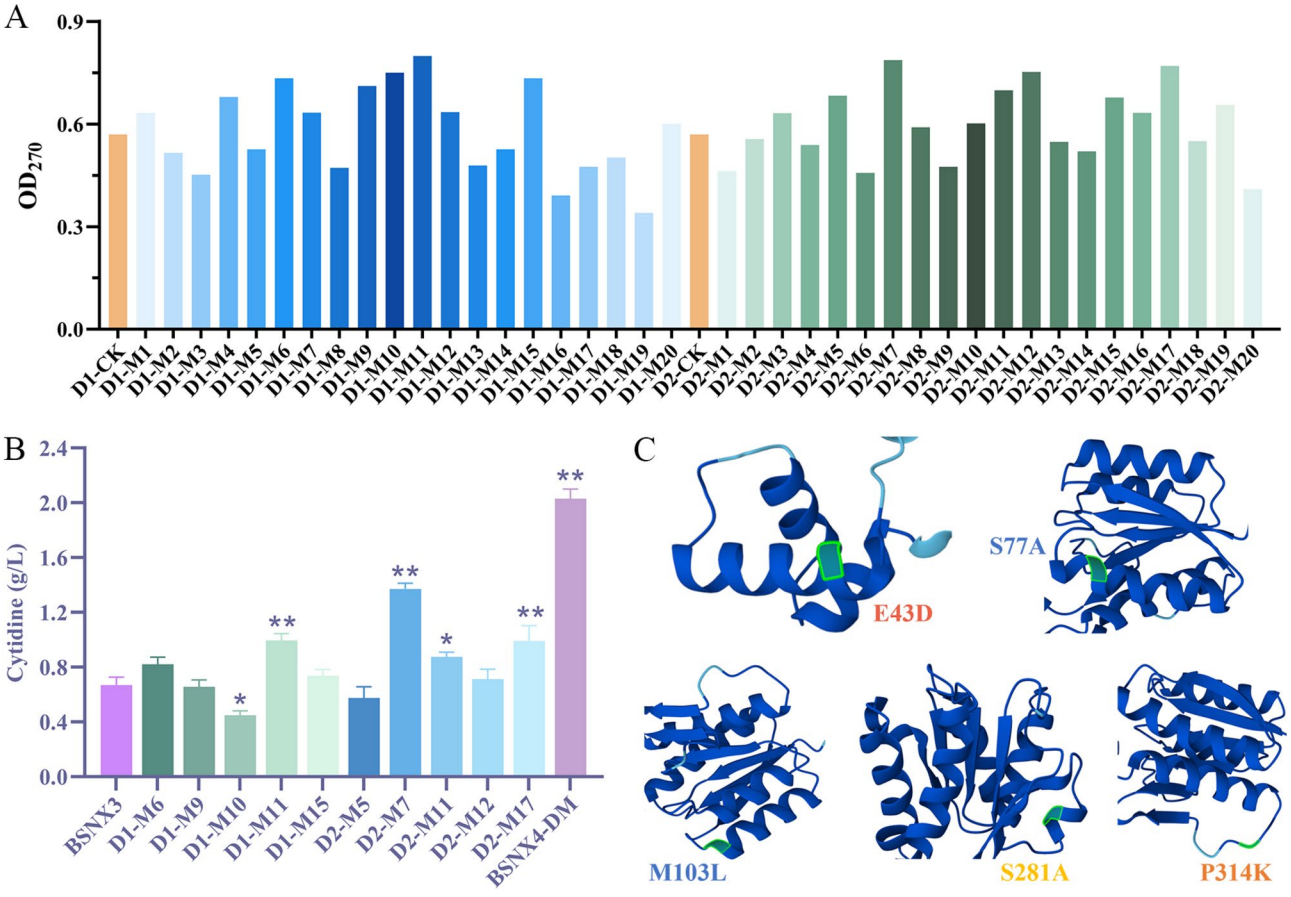

Fig. 3 Mutation library construction of CcpA. (**A**) The top 40 mutants with the highest absorbance at 270 nm were screened from the CcpA mutant library by high-throughput screening. (**B**) The cytidine titers of the screened mutant libraries D1 (E43D) and D2 (S77A/M103L/S281A/P314K), and the combined mutant BSNX4-DM of the two domains (E43D/S77A/M103L/S281A/P314K). (**C**) In the wild-type CcpA domain D1, the residue E at position 34 was mutated to D. In domain D2, the residue S at position 77 is mutated to A; the residue M at position 103 is mutated to L; the residue S at position 281 is mutated to A; and the residue P at position 314 is mutated to K

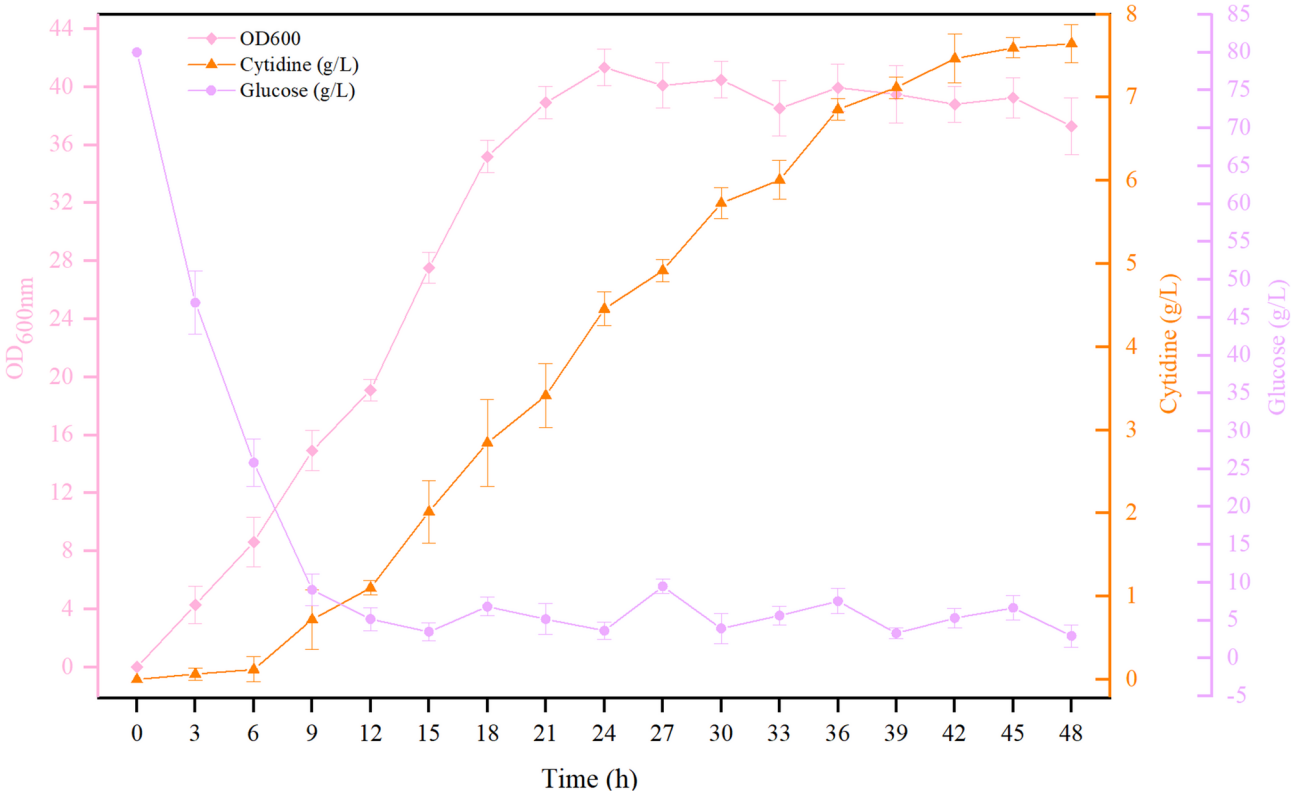

Fig. 4 Fed-batch production of cytidine using BSNX4-DM in a 5-L bioreactor. The time courses of cytidine titer, cell growth curves, and glucose concentration are presented. The maximum OD_{600} value was 41.34, the cytidine titer was 7.65 g/L, and the cytidine yield was 0.06 g/g glucose

9 h, and the titer reached 7.65 g/L at 48 h, which was 3.77-fold that of the shake flask culture titer (2.03 g/L). A cytidine yield and productivity of 0.06 g/g glucose and 0.16 g/L/h, respectively, were achieved. During the fermentation process, the concentration of glucose was controlled around 5 g/L.

Multi-omics analysis of the effects of PyrR and CcpA modifications on cytidine biosynthesis

With the advancement of multi-omics technology, there is a growing shift towards comprehensive system-level analyses instead of isolated decomposition studies [37]. Transcriptomics explores gene expression and transcriptional regulation at the RNA level, while metabolomics extends this approach by revealing the mechanism through which metabolic changes influence biological activities and affect phenotypes [38, 39]. In recent years, studies integrating transcriptomic and metabolomic data have emerged as a key component of systems biology research, revealing the state of post-transcriptional regulation. Therefore, this combined transcriptomics and metabolomics to analyze the metabolic pathways (central carbon metabolism, nitrogen metabolism, nucleotide metabolism, and amino acid metabolism) that directly or indirectly affect cytidine biosynthesis after the modification of PyrR and CcpA in *B. subtilis*.

Transcriptome analysis of PyrR and CcpA-modified strains

To explore the effects of PyrR and CcpA on cytidine synthesis at the gene level, the transcriptomes of the strains BSNX2, BSNX3, and BSNX4-DM were analyzed. As shown in Fig. 5A, compared with the control strain BSNX2, 693 DEGs (up-regulated: 371; down-regulated: 322) emerged in the BSNX3 strain when *pyrR* was knocked out. These genes were mainly enriched in protein metabolic processes, organic nitrogen compound metabolic processes, ribosomes, cells, and the structural constituents of ribosomes (Fig. 6B). KEGG pathway enrichment analysis revealed that these DEGs were mainly enriched in ribosomes, pyrimidine metabolism, non-ribosomal peptide structures, nitrogen metabolism, and valine, leucine, and isoleucine biosynthesis (Fig. 6C). These results indicated that *pyrR* knockout triggers nucleotide metabolism.

The CcpA mutant contained 1396 DEGs (up-regulated: 685; down-regulated: 711) (Fig. 5B). GO enrichment analysis showed that the DEGs were mainly enriched in nucleoside metabolic processes, carbohydrate transport, the phosphoenolpyruvate-dependent sugar phosphotransferase system, and oxidation-reduction processes (Fig. 6C). KEGG pathway enrichment analysis showed that the DEGs were mainly enriched in carbon metabolism (PTS system, glycolysis/gluconeogenesis,

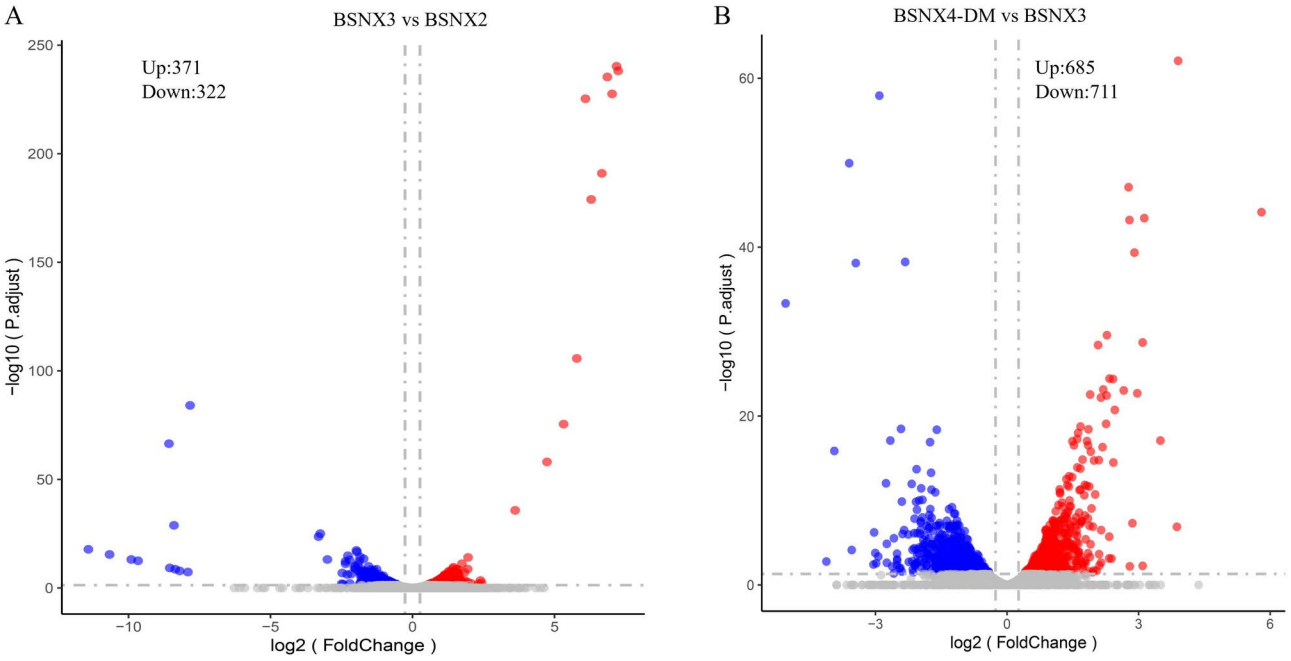

Fig. 5 Transcriptome analysis of PyrR and CcpA-modified strains. (**A**) (**B**) Volcanic map of DEGs

pyruvate metabolism, C5-branched dibasic acid metabolism, TCA cycle), nitrogen metabolism, nucleotide metabolism (pyrimidine metabolism, purine metabolism), and amino acid metabolism (alanine, aspartate and glutamate metabolism, valine, leucine and isoleucine biosynthesis) (Fig. 6D). These data demonstrated that CcpA modification triggers pathways associated with carbon, nucleotide, nitrogen, and amino acid metabolism.

Metabolome analysis of PyrR and CcpA-modified strains

To detect the metabolite changes induced by the modification of the TFs PyrR and CcpA, metabolomics analysis was performed in strains BSNX2, BSNX3, and BSNX4-DM. In contrast to the control strain BSNX2, there were 798 significantly up-regulated and 436 significantly down-regulated differential metabolites (DMs) in the PyrR knockout strain BSNX3 (Fig. 7A). According to KEGG pathway enrichment, the top three pathways associated with these metabolites were nucleotide metabolism, pyrimidine metabolism, and purine metabolism (Fig. 7B). A total of 1190 significantly up-regulated and 1372 significantly down-regulated DMs were identified in the CcpA mutant strain BSNX4-DM (Fig. 7C). These DMs were mainly enriched in nucleotide metabolism (Pyrimidine metabolism, Purine metabolism), carbon metabolism (Glycolysis, Pyruvate metabolism, TCA cycle, Pantothenate and CoA biosynthesis, Pentose phosphate pathway, Propanoate metabolism) and amino acid metabolism (Glycine, serine and threonine metabolism, Arginine and proline metabolism, Biosynthesis of amino acids, Valine, leucine and isoleucine biosynthesis, Histidine metabolism,) pathways (Fig. 7D). Thus, the results of combined transcriptomics and metabolomics revealed that central carbon metabolism, nitrogen metabolism, nucleotide metabolism, and amino acid metabolism were considerably altered after PyrR and CcpA modification.

Key metabolic pathways in PyrR and CcpA-modified strains revealed by multi-omics

Nucleotide metabolism Nucleotide metabolism mainly involves a *de novo* synthesis pathway and a salvage synthesis pathway. The *de novo* synthesis pathway, which uses aspartic acid, glutamine, PRPP, and HCO_3^- as raw materials, is the main pathway generating nucleotides through a series of enzymatic reactions [7]. Specific nodes in the *de novo* synthesis pathway of pyrimidine nucleosides are strictly regulated by the regulatory factor PyrR via effectors such as uridine-5'-monophosphate (UMP), uridine-5'-diphosphate (UDP), UTP, and PRPP [19, 45]. As shown in Fig. 8, most genes associated with the pyrimidine metabolic pathway (*pyrAA*, *pyrAB*, *pyrB*, *pyrC*, *pyrD*, *pyrE*, *pyrF*, *pyrK*, *pdp*, *yfkN*, *cmk* and *ndk*) were significantly up-regulated in the PyrR knockout strain, and only *nrdE*, *tmk*, and *carA* were down-regulated, consistent with the RT-qPCR results. The genes involved in purine metabolism pathway (*purA*, *purF*, *purH*, *purN*, *purN*) were significantly down-regulated. Metabolomics data showed that four metabolites from the pyrimidine metabolic pathway (UMP, Orotidine-5'-phosphate (OMP), UDP, Cytidine, Cytosine) were significantly up-regulated, while three from the purine metabolic pathway (adenosine, guano-

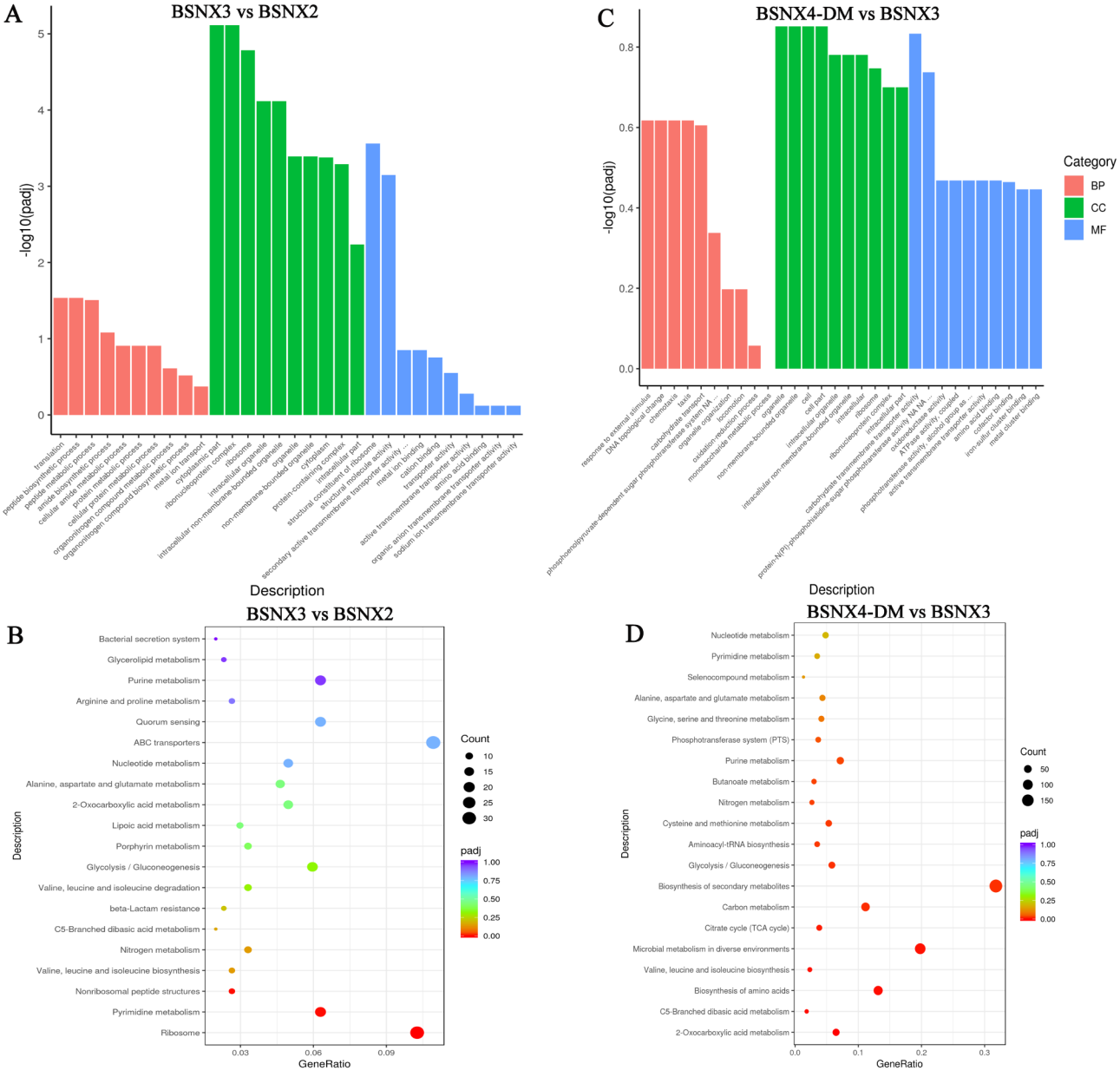

Fig. 6 Transcriptome analysis of PyrR and CcpA-modified strains. (**A**) (**C**) GO enrichment of DEGs. (**B**) (**D**) KEGG enrichment of DEGs. padj (adjusted *p*-value)

sine, adenine, allantoic acid) were significantly down-regulated, in line with the transcriptomics data. These results showed that knocking out the TF PyrR can increase the expression of genes involved in the *de novo* synthesis pathway of pyrimidine nucleosides, thus promoting cytidine synthesis.

In the CcpA mutant, the pyrimidine metabolism-related genes *pyrE*, *pyrF*, *pyrAB*, *pyrK*, *pyrD*, *pyrAA*, *pyrC*, *nrdE*, *pyrB*, *ndk*, *pdp*, *pdeB*, and *yfkN* were significantly up-regulated, whereas the genes *nrdF*, *upp*, *carA*, *thyB*, *tmk*, and *dck* were significantly down-regulated. This led to an increase in the levels of OMP, UMP, UDP, cytidine-5'-diphosphate (CDP), cytidine-5'-monophosphate (CMP), cytidine, cytosine, and uracil, and a corresponding decrease in the contents of deoxyuridine (Fig. 8). Moreover, except for *purB*, *purC*, *guaA*, and *guaB*, all other genes associated with the purine metabolic pathway were significantly down-regulated, leading to a decrease in the levels of the corresponding purine nucleosides (Adenosine, Guanosine, Adenine) (Fig. 8). These results demonstrate that CcpA modification can increase the expression of pyrimidine metabolic pathway-related genes, thus promoting cytidine production. In future studies, the direction of metabolic flow could be changed by modifying CcpA to increase the expression

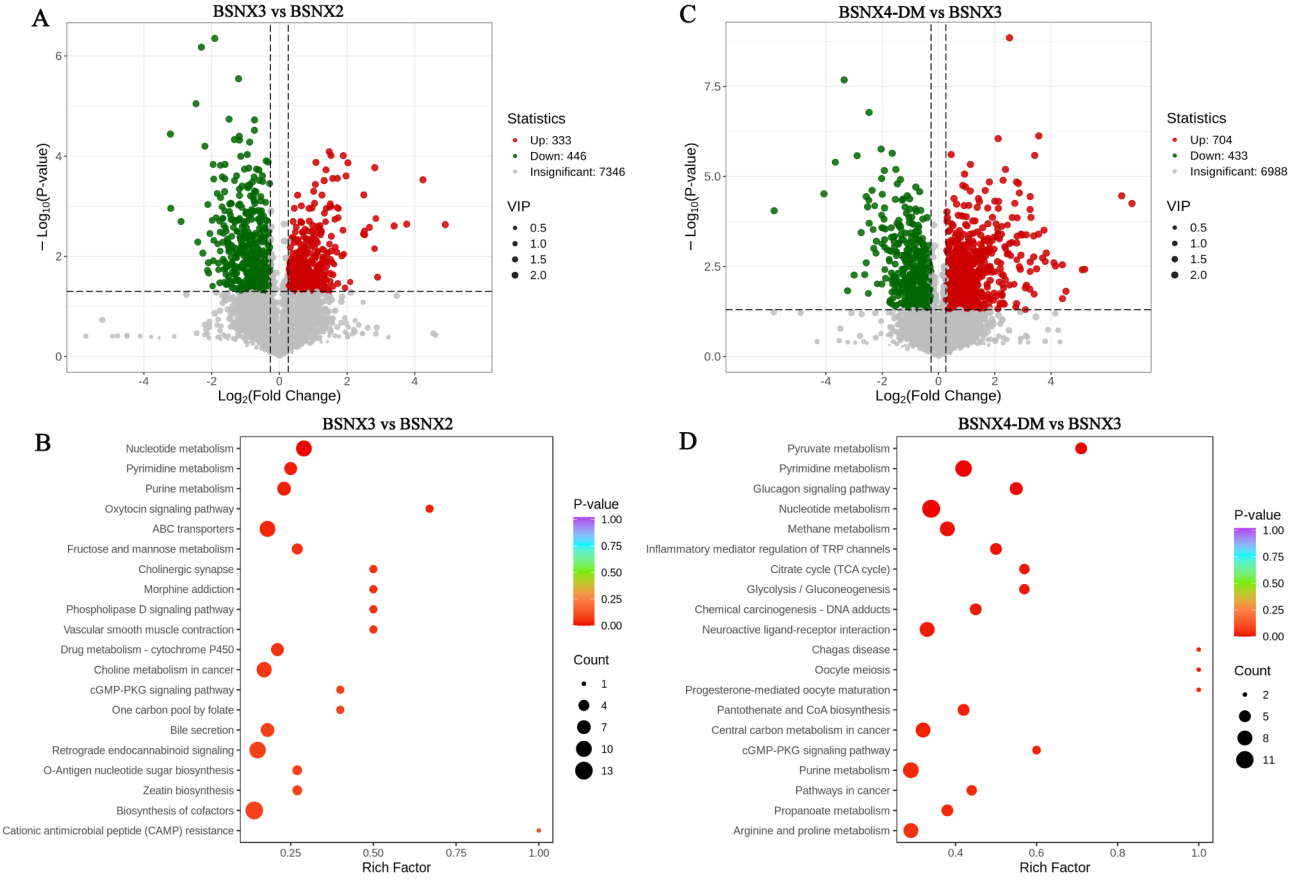

Fig. 7 Metabolome analysis of PyrR and CcpA-modified strains. (**A**) (**C**) Volcanic map of DMs. (**B**) (**D**) KEGG enrichment of DMs

of *de novo* pyrimidine nucleoside synthesis pathway genes, thus further boosting the biosynthesis of these nucleosides.

Carbon metabolism In *B. subtilis*, central carbon metabolism provides the key precursors and energy required for the *de novo* synthesis of cytidine [7, 10]. The PTS system, glycolysis, TCA cycle, and PP pathway are the main components of the carbon metabolism network. Studies have demonstrated that the genes related to the transport and utilization of carbon sources in *B. subtilis* are strictly regulated by CcpA via effectors such as fructose-1, 6-diphosphate (FBP) to achieve optimal intracellular carbon metabolism flow [21, 46]. As shown in Fig. 8, in the CcpA mutant strain, the genes related to the PTS system (*sacP*, *bglP*, *ptsJ*, *ptsG*, *ptsH*, *gamP*, *malP*) were all significantly up-regulated, increasing the utilization of phosphoenolpyruvate (PEP) and promoting glucose transport. Thus, the contents of glucose, glucose-6-phosphate (G6P) and fructose-6-phosphate (F6P) increased and those of PEP decreased. Among the genes related to glycolysis *glcK*, *pgi*, *gapA*, *gapB*, *pdhA*, *pdhB*, *pdhC*, *pdhD*, *pckA* and *acsA* were up-regulated, while *pfkA*, *fbaA*, *pgk*, *pgm*, *eno*, *pyk*, *ackA* and *pta* were down-regulated, leading to a decrease in dihydroxyacetone phosphate (DHAP) and acetate. Additionally, the content of acetyl-CoA dropped below detectable levels. Except for *icd*, the other genes associated with the TCA cycle were significantly up-regulated. As a result, the content of pyruvic acid (PYR), malic acid (MAL) and succinic acid (SUCC) decreased, and α-ketoglutarate (α-KG) and isocitric acid (ICIT) were increased, while oxaloacetate (OAA) was not detected. All key genes linked to the PP pathway (*zwf*, *pgl*, *gndA*, *gntZ*, *rpe*, *prs*, *ycdF*) were significantly up-regulated, and only *tktA* and *rpiB* were down-regulated. This resulted in decreased 2-phospho-glyceric acid (2PG) levels and increased gluconic acid (GA), ribulose 5-phosphate (Ru5P), xylulose 5-phosphate (Xu5P), ribose-5-phosphate (R5P) and 5-phosphoribosyl-1α-pyrophosphate (PRPP) levels. However, since metabolism is inherently post-transcriptional, changes in gene expression and metabolite content are not typically synchronized. Hence, the same substance may exhibit different trends at different omics levels.

Overall, the results indicated that the modification of the TF CcpA can alter the transcription of genes associated with the PTS system, glycolysis, TCA cycle, and PP pathway, shifting the metabolic flux toward pyrimidine

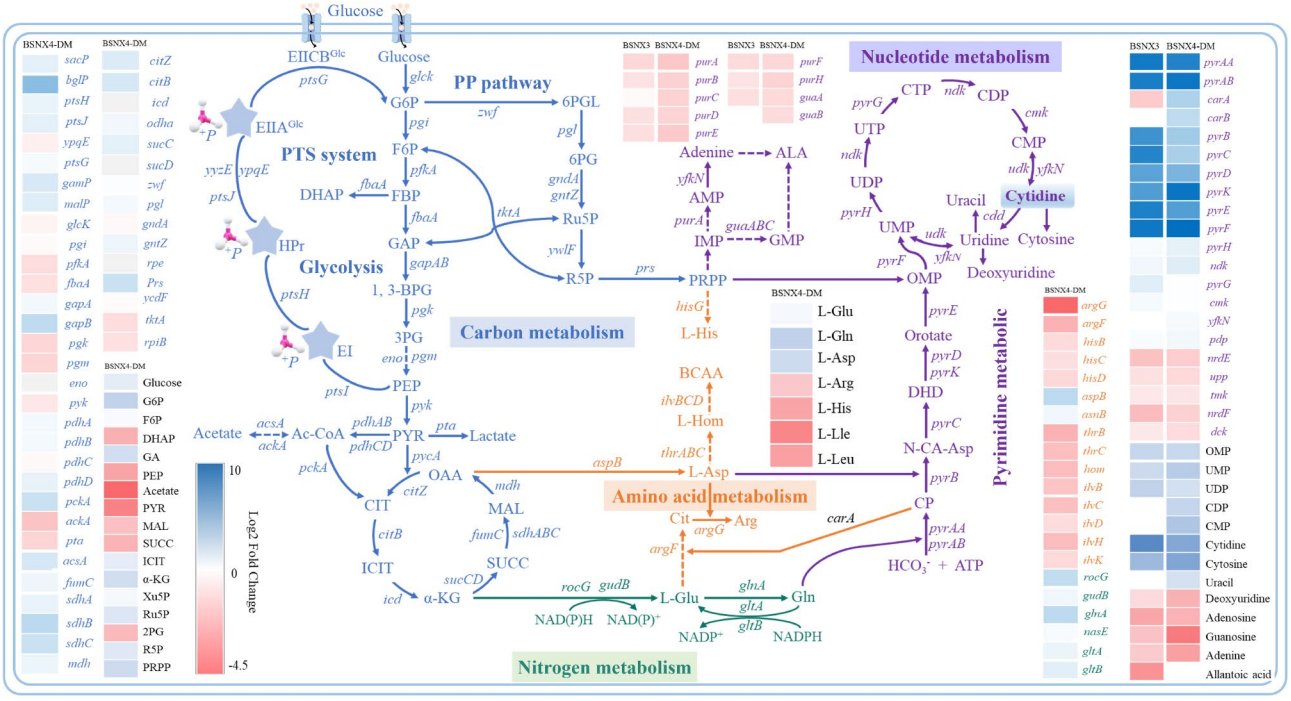

Fig. 8 Comparison of multi-omics data in cytidine biosynthesis networks. The DEGs and DMs related to nucleotide metabolism, carbon metabolism, nitrogen metabolism and amino acid metabolism in recombinant strains were analyzed (Details in Supplementary file 2). Abbreviations: G6P, glucose-6-phosphate; F6P, fructose-6-phosphate; FBP, fructose-1,6-bisphosphate; DHAP, dihydroxyacetone phosphate; GAP, glyceraldehyde-3-phosphate; 1,3-BPG, glycerate 1,3-diphosphate; 3PG, 3-phosphoglycerate; GA, gluconic acid; PEP, phosphoenolpyruvate; PYR, pyruvic acid; OAA, oxaloacetate; MAL, malic acid; SUCC, succinic acid; α-KG, α-ketoglutaric acid; ICIT, isocitrate; CIT, citrate; 6PGL, 6-phosphogluconolactone; 6PG, 6-phosphogluconic acid; RU5P, ribulose 5-phosphate; R5P, ribose 5-phosphate; PRPP, 5-phosphoribosyl-1α-pyrophosphate; IMP, inosinemonphosphate; AMP, adenosine 5′-monophosphate; GMP, guanosine monophosphate; ALA, allantoic acid; L-Glu, L-glutamate; Gln, glutamine; Cit, citrulline; Arg, arginase; L-Asp, L-asparaginase; L-Hom, L-homoserine; L-His, L-histidine; BCAA, branched-chain amino acid; CP, carbamoyl phosphate; N-CA-Asp, N-carbamoyl aspartate; DHD, dihydroorotate; OMP, orotidine 5′-phosphate; UMP, uridine monophosphate; UDP, uridine diphosphate; UTP, uridine triphosphate; CTP, cytidine triphosphate; CDP, cytidine diphosphate; CMP, cytidine monophosphate

metabolic pathways and increasing the expression of *de novo* pyrimidine nucleoside synthesis pathway genes. Thus, this alteration ultimately promotes the biosynthesis of cytidine. The overexpression of genes associated with the PP pathway (e.g. *zwf*, *gnd*, *ykgB* and *prs*) is widely used as a strategy to construct pyrimidine nucleoside-producing strains [11, 47]. However, the modification of genes related to the PTS system, glycolysis and TCA cycle (e.g. *ptsG*, *ptsH*, *ptsI*, *glcK*, *gapA*, *pycA*, *pdhA*, *citZ*, *citB* and *ackA*) has rarely been performed to enhance pyrimidine nucleoside accumulation. Therefore, these genes may serve as potential candidates for improving pyrimidine nucleoside production in the future.

Nitrogen metabolism As a key component of biological macromolecules (nucleic acids and proteins), nitrogen also serves as an essential element for microbial growth and is essential for development and information exchange in microorganisms [48]. However, nitrogen assimilation mainly occurs via the GDH assimilation pathway and GS/GOGAT assimilation pathway, which synthesize glutamate and glutamine — the two main nitrogen donors in microbial cells [49]. In *B. subtilis*, GDH, GS, and GOGAT are encoded by the genes *rocG*/*gudB*, *glnA* and *gltAB*, respectively. The combination of our transcriptomic and metabolomic data showed that the nitrogen metabolism-related genes *rocG*, *gudB*, *glnA*, *nasE*, *gltA* and *gltB* genes were significantly up-regulated after CcpA modification, and the contents of L-glutamate and L-glutamine were increased (Fig. 8). Hence, CcpA modification also seemed to affect nitrogen metabolism, especially the pathways involved in the biosynthesis of glutamate and glutamine, leading to cytidine accumulation.

Amino acid metabolism In addition to being the basic units of protein, amino acids also act as important precursors of nucleotide biosynthesis [7, 50]. In addition, the one-carbon unit (methyl, methylene, methenyl, methynyl, cresol and iminomethyl) produced via the catabolism of some amino acids serves as a key synthetic raw material for purine and pyrimidine and represents the link between amino acids and nucleotides [51]. In our study, in the CcpA mutant strain, the expression of genes associated with the L-aspartate synthesis pathway (*aspB*, *asnB*) was up-regu-

lated, leading to an increase in the content of L-aspartate. However, arginine, histidine, and branched-chain amino acid biosynthesis pathway-related genes (*argGF*, *hisBCD*, *thrBC*, *ilvBCDHK*) were significantly down-regulated, resulting in decreased levels of the corresponding amino acids (L-Arg, L-His, L-Lle, L-Leu) (Fig. 8). These results demonstrated that the increase in cytidine production in the CcpA mutant strains could be directly related to the attenuated activity of these branched metabolic pathways.

Conclusion

This study showed that knockout of the *pyrR* can effectively alleviate its transcriptional repression of the pyr operon and promote cytidine synthesis. Subsequently, the *ccpA* mutant library was constructed, and the mutant BSNX4-DM was screened to increase the cytidine titer to 2.03 g/L in shake flask fermentation. Finally, fed-batch fermentation in a 5 L fermenter reached a cytidine titer of 7.65 g/L. Through multi-omics analysis, it was found that the expression levels of pyrimidine metabolic pathway genes and metabolites in *pyrR* knockout strains increased, and the expression of purine metabolic pathway genes and metabolites was down-regulated. However, in *ccpA* mutant, the pyrimidine metabolic pathway was enhanced, and the expression of most genes in the purine metabolic pathway was decreased. The related genes of PTS system were significantly up-regulated, and glucose transport was accelerated. The expression of genes related to TCA cycle and PP pathway was up-regulated, and the metabolic flow turned to pyrimidine nucleoside synthesis pathway. The synthesis fluxes of glutamine and aspartic acid increased, and the synthesis pathways of arginine, histidine and branched-chain amino acids decreased, which led to an increase in the supply of cytidine synthesis precursors. However, the biosynthesis of cytidine involves complex regulatory networks, and the regulatory mechanism of mutant CcpA on the global metabolic flow of *B. subtilis* needs to be further elucidated in future studies. Overall, these strategies help to optimizing the overall transcription level of intracellular carbon-nitrogen metabolic networks, and could be combined with systems metabolic engineering methods for constructing more efficient microbial cell factories in the future.

Abbreviations

CcpA	Catabolite control protein A
TCA	Tricarboxylic acid
PTS	Phosphotransferase
PP	Pentose phosphate
TFs	Transcription factors
BLs	Binding loops
PRPP	5-phosphoribosyl-1α-pyrophosphate
SCFA	Short-chain fatty acid
GDH	Glutamate dehydrogenase
GOGAT	Glutamate synthase
GS	Glutamine synthetase
DEGs	Differentially expressed genes
GO	Gene Ontology
KEGG	Kyoto encyclopedia of genes and genomes
RT-qPCR	Real-time quantitative PCR
HPLC	High-performance liquid chromatography
DBD	DNA-binding domain
DEBD	Dimerization effect binding domain
HTH	Helix-turn-helix motif
cre	Catabolite-responsive elements
DMs	Differential metabolites
UDP	Uridine-5′-diphosphate
UMP	Uridine-5′-monophosphate
CDP	Cytidine-5′-diphosphate
CMP	Cytidine-5′-monophosphate
FBP	Fructose-1, 6-diphosphate
PEP	Phosphoenolpyruvate
G6P	Glucose-6-phosphate
F6P	Fructose-6-phosphate
DHAP	Dihydroxyacetone phosphate
GA	Gluconic acid
PYR	Pyruvic acid
MAL	Malic acid
SUCC	Succinic acid
OAA	Oxaloacetate
α-KG	α-Ketoglutarate
2PG	2-Phospho-glyceric acid
Ru5P	Ribulose 5-phosphate
Xu5P	Xylulose 5-phosphate
R5P	Ribose-5-phosphate

Supplementary Information

The online version contains supplementary material available at https://doi.org/10.1186/s12934-025-02731-y.

Supplementary Material 1: **Supplementary Table 1**. Primers used in this study.

Supplementary Material 2

Acknowledgements

Not applicable.

Author contributions

XJZ: Writing– original draft, Methodology, Data curation, Validation. LL, PLN, TY: Methodology, Visualization, Software. WD, XBW, JNX: Formal analysis, Supervision, Investigation. HTF, HYL: Project administration, Writing– review and editing, Resources, Funding acquisition.

Funding

This work was supported by the National Natural Science Foundation, China (31860020), Ningxia Natural Science Foundation Project (2023AAC02030), the Ningxia Hui Autonomous Region Youth Top Talent Training Project (022004000010), the Key Research and Development Program of Yinchuan (2023NYHZC01, 2024NYHZC002), Industry-University-Research collaboration of Zhuhai (No. 2220004002701), Helanshan Scholars Program of Ningxia University.

Data availability

Data is provided within the manuscript or supplementary information files.

Declarations

Ethics approval and consent to participate

Not applicable.

Consent for publication

Not applicable.

Competing interests
The authors declare no competing interests.

Author details
[1]School of Life Science, Ningxia University, Yinchuan 750021, Ningxia, China
[2]School of Food Science and Engineering, Ningxia Key Laboratory for Food Microbial- Applications Technology and Safety Control, Ningxia University, Yinchuan 750021, Ningxia, China

Received: 16 November 2024 / Accepted: 25 April 2025
Published online: 13 May 2025

References

1. Wang X, Xiao Y, Cui Z, Li Z, Li L, Wu L, et al. Cyclocytidine hydrochloride inhibits the synthesis of relaxed circular DNA of hepatitis B virus. PeerJ. 2022;10:e13719.
2. Salehi B, Selamoglu Z, Mileski S, Pezzani K, Redaelli R, Cho M. Liposomal cytarabine as cancer therapy: from chemistry to medicine. Biomolecules. 2019;9:773.
3. Synoradzki K, Grieb P. Citicoline: a superior form of Choline?? Nutrients. 2019;11:1569.
4. Zhang X, Liu L, Ma C, Zhang H, Liu H, Fang H. Improving the level of the cytidine biosynthesis in *E. coli* through atmospheric room temperature plasma mutagenesis and metabolic engineering. J Appl Microbiol. 2024;135:lxae133.
5. Zhu H, Yang SM, Yuan ZM, Ban R. Metabolic and genetic factors affecting the productivity of pyrimidine nucleoside in *Bacillus subtilis*. Microb Cell Fact. 2015;14:54.
6. Fang H, Liu H, Chen N, Zhang C, Xie X, Xu Q. Site-directed mutagenesis studies on the uridine monophosphate binding sites of feedback Inhibition in carbamoyl phosphate synthetase and effects on cytidine production by *Bacillus amyloliquefaciens*. Can J Microbiol. 2013;59:374–9.
7. Zhang X, Niu P, Liu H, Fang H. Production of pyrimidine nucleosides in microbial systems via metabolic engineering: theoretical analysis research and prospects. Biotechnol Adv. 2024;75:108419.
8. Nielsen J, Keasling JD. Eng Cell Metabolism Cell. 2016;164:1185–97.
9. Han B, Dai Z, Li Z. Computer-Based design of a cell factory for High-Yield cytidine production. ACS Synth Biol. 2022;11:4123–33.
10. Yang K, Li Z. Multistep construction of metabolically engineered *Escherichia coli* for enhanced cytidine biosynthesis. Biochem Eng J. 2020;154:107433.
11. Fang H, Xie X, Xu Q, Zhang C, Chen N. Enhancement of cytidine production by coexpression of *gnd*, *zwf*, and *prs* genes in recombinant *Escherichia coli* CYT15. Biotechnol Lett. 2013;35:245–251.
12. Ma R, Fang H, Liu H, Pan L, Wang H, Zhang H. Overexpression of uracil permease and nucleoside transporter from *Bacillus amyloliquefaciens* improves cytidine production in *Escherichia coli*. Biotechnol Lett. 2021;43:1211–9.
13. Kim JS, Koo BS, Hyun HH, Lee HC. Deoxycytidine production by a metabolically engineered *Escherichia coli* strain. Microb Cell Fact. 2015;14:98.
14. Wang Y, Bai C, Ruan Y, Liu M, Chu Q, Qiu L, et al. Coordinative metabolism of glutamine carbon and nitrogen in proliferating cancer cells under hypoxia. Nat Commun. 2019;10:201.
15. Yamamoto J, Chumsakul O, Toya Y, Morimoto T, Liu S, Masuda K, et al. Constitutive expression of the global regulator AbrB restores the growth defect of a genome-reduced *Bacillus subtilis* strain and improves its metabolite production. DNA Res. 2022;29:dsac015.
16. Xie CY, Li WJ, Feng H. Tuning transcription factor DegU for developing extracellular protease overproducer in *Bacillus pumilus*. Microb Cell Fact. 2023;22:163.
17. Tolibia SEM, Pacheco AD, Balbuena SYG, Rocha J, López Y, López VE. Engineering of global transcription factors in *Bacillus*, a genetic tool for increasing product yields: a bioprocess overview. World J Microbiol Biotechnol. 2022;39:12.
18. Deng C, Lv X, Li J, Zhang H, Liu Y, Du G, et al. Synergistic improvement of N-acetylglucosamine production by engineering transcription factors and balancing redox cofactors. Metab Eng. 2021;67:330–46.
19. Turnbough CL Jr., Switzer RL. Regulation of pyrimidine biosynthetic gene expression in bacteria: repression without repressors. Microbiol Mol Biol Rev. 2008;72:266–300.
20. Wang Y, Ma R, Liu L, He L, Ban R. Improvement of uridine production in *Bacillus subtilis* by metabolic engineering. Biotechnol Lett. 2018;40:151–5.
21. Blencke HM, Homuth G, Ludwig H, Mader U, Hecker M, Stulke J. Transcriptional profiling of gene expression in response to glucose in *Bacillus subtilis*: regulation of the central metabolic pathways. Metab Eng. 2003;5:133–49.
22. Schumacher MA, Sprehe M, Bartholomae M, Hillen W, Brennan RG. Structures of carbon catabolite protein A-(HPr-Ser46-P) bound to diverse catabolite response element sites reveal the basis for high-affinity binding to degenerate DNA operators. Nucleic Acids Res. 2011;39:2931–42.
23. Zhang Y, Xiao F, Zhang L, Ding Z, Shi G, Li Y. A new mechanism of carbon metabolism and acetic acid balance regulated by CcpA. Microorganisms. 2023;11:2303.
24. Wacker I, Ludwig H, Reif I, Blencke HM, Detsch C, Stülke J. The regulatory link between carbon and nitrogen metabolism in *Bacillus subtilis*: regulation of the GltAB Operon by the catabolite control protein CcpA. Microbiol (Reading). 2003;149:3001–9.
25. Anagnostopoulos C, Spizizen J. Requirements for transformation in *Bacillus Subtilis*. J Bacteriol. 1961;81:741–6.
26. Jin L, Li L, Zhou L, Zhang R, Xu Y, Li J. Improving expression of bovine lactoferrin n-lobe by promoter optimization and codon engineering in *Bacillus subtilis* and its antibacterial activity. J Agric Food Chem. 2019;67:9749–56.
27. Altenbuchner J. Editing of the *Bacillus subtilis* genome by the CRISPR-Cas9 system. Appl Environ Microbiol. 2016;82:5421–7.
28. Ferrando J, Filluelo O, Zeigler DR, Picart P. Barriers to simultaneous multilocus integration in *Bacillus subtilis* tumble down: development of a straightforward screening method for the colorimetric detection of one-step multiple gene insertion using the CRISPR-Cas9 system. Microb Cell Fact. 2023;22:21.
29. Bailey TL, Boden M, Buske FA, Frith M, Grant CE, Clementi L, et al. MEME SUITE: tools for motif discovery and searching. Nucleic Acids Res. 2009;37:W202–8.
30. Fan X, Wu H, Li G, Yuan H, Zhang H, Li Y, et al. Improvement of uridine production of *Bacillus subtilis* by atmospheric and room temperature plasma mutagenesis and high-throughput screening. PLoS ONE. 2017;12:e0176545.
31. Anders S, Huber W. Differential expression of RNA-Seq data at the gene level–the DESeq package. Heidelberg, Germany: European Molecular Biology Laboratory (EMBL); 2012;10:f1000research.
32. Love MI, Huber W, Anders S. Moderated Estimation of fold change and dispersion for RNA-seq data with DESeq2. Genome Biol. 2014;15:550.
33. Chambers MC, Maclean B, Burke R, Amodei D, Ruderman DL, Neumann S, et al. A cross-platform toolkit for mass spectrometry and proteomics. Nat Biotechnol. 2012;30:918–20.
34. Smith CA, Want EJ, O'Maille G, Abagyan R, Siuzdak G. XCMS: processing mass spectrometry data for metabolite profiling using nonlinear peak alignment, matching, and identification. Anal Chem. 2006;78:779–87.
35. Livak KJ, Schmittgen TDJ. Analysis of relative gene expression data using real-time quantitative PCR and the $2^{-\Delta\Delta CT}$ method. 2001;25:402–8.
36. Marchler-Bauer A, Derbyshire MK, Gonzales NR, Lu S, Chitsaz F, Geer LY, et al. CDD: NCBI's conserved domain database. Nucleic Acids Res. 2015;43:D222–6.
37. Schumacher MA, Allen GS, Diel M, Seidel G, Hillen W, Brennan RG. Structural basis for allosteric control of the transcription regulator CcpA by the phosphoprotein HPr-Ser46-P. Cell. 2004;118:731–41.
38. Gorke B, Stulke J. Carbon catabolite repression in bacteria: many ways to make the most out of nutrients. Nat Rev Microbiol. 2008;6:613–24.
39. Schumacher MA, Seidel G, Hillen W, Brennan RG. Phosphoprotein Crh-Ser46-P displays altered binding to CcpA to effect carbon catabolite regulation. J Biol Chem. 2006;281:6793–800.
40. Deutscher J. The mechanisms of carbon catabolite repression in bacteria. Curr Opin Microbiol. 2008;11:87–93.
41. Stulke J, Hillen W. Regulation of carbon catabolism in *Bacillus species*. Annu Rev Microbiol. 2000;54:849–80.
42. Miwa Y, Nakata A, Ogiwara A, Yamamoto M, Fujita Y. Evaluation and characterization of catabolite-responsive elements (cre) of *Bacillus subtilis*. Nucleic Acids Res. 2000;28:1206–10.
43. Zalieckas JM, Wray LV Jr, Ferson AE, Fisher SH. Transcription-repair coupling factor is involved in carbon catabolite repression of the *Bacillus subtilis* hut and Gnt operons. Mol Microbiol. 1998;27:1031–8.
44. Miwa Y, Fujita Y. Involvement of two distinct catabolite-responsive elements in catabolite repression of the *Bacillus subtilis* myo-inositol (iol) Operon. J Bacteriol. 2001;183:5877–84.
45. Hove-Jensen B, Andersen KR, Kilstrup M, Martinussen J, Switzer RL, Willemoes M. Phosphoribosyl diphosphate (PRPP): biosynthesis, enzymology, utilization, and metabolic significance. Microbiol Mol Biol Rev. 2017;81:e00040–16.
46. Fujita Y. Carbon catabolite control of the metabolic network in *Bacillus subtilis*. Biosci Biotechnol Biochem. 2009;73:245–59.

47. Wang C, Xu J, Ban R. Metabolic engineering of *Bacillus subtilis* for high-level production of uridine from glucose. Lett Appl Microbiol. 2022;75:824–30.
48. Jenkins VA, Barton GR, Robertson BD, Williams KJ. Genome wide analysis of the complete GlnR nitrogen-response Regulon in *Mycobacterium smegmatis*. BMC Genomics. 2013;14:301.
49. Han F, Zhou W. Nitrogen recovery from wastewater by microbial assimilation - a review. Bioresour Technol. 2022;363:127933.
50. Motter J, Benckendorff CMM, Westarp S, Sunde-Brown P, Neubauer P, Kurreck A, et al. Purine nucleoside antibiotics: recent synthetic advances Harnessing chemistry and biology. Nat Prod Rep. 2024;41:873–84.
51. Petrova B, Maynard AG, Wang P, Kanarek N. Regulatory mechanisms of one-carbon metabolism enzymes. J Biol Chem. 2023;299:105457.

Publisher's note